

Babbling brook to thunderous torrent: Using sound to monitor river stage

Wm. Alexander Osborne¹  | Rebecca A. Hodge¹  | Gordon D. Love²  | Peter Hawkin³ | Ruth E. Hawkin³

¹Department of Geography, Durham University, Durham, UK

²Departments of Computer Science and Physics, Durham University, Durham, UK

³Evolto, The Water Tower, Station Court, Haltwhistle, Northumberland, UK

Correspondence

William Alexander Osborne, Department of Geography, Durham University, Durham DH1 3LE, UK.

Email: william.a.osborne@durham.ac.uk

Funding information

European Regional Development Fund, Grant/Award Number: 25R17P01847

Abstract

The passive, ambient sound above the water from a river has previously untapped potential for determining flow characteristics such as stage. Measuring sub-aerial sound could provide a new, efficient way to continuously monitor river stage, without the need for in-stream infrastructure. Previous published work has suggested that there might be a relationship between sound and river stage, but the analysis has been restricted to a narrow range of flow conditions and river morphologies. We present a method to determine site suitability and the process of how to record and analyse sound. Data collected along a 500 m length of the River Washburn during July 2019 is used to determine what makes a site suitable for sound monitoring. We found that sound is controlled by roughness elements in the channel, such as a boulder or weir, which influences the sound produced. On the basis of these findings, we collect audio recordings from six sites around the northeast of England, covering a range of flow conditions and different roughness elements, since 2019. We use data from those sites collected during storms Ciara and Dennis to produce a relationship between this sound and river stage. Our analysis has shown a positive relationship between an R^2 of 0.73 and 0.99 in all rivers, but requires careful site selection and data processing to achieve the best results. We introduce a filter that is capable of isolating a river's sound from other environmental sound. Future work in examining the role of these roughness elements is required to understand the full extent of this technique. By demonstrating that sound can operate as a hydrometric tool, we suggest that sound monitoring could be used to provide cost-effective monitoring devices, either to detect relative change in a river or, after more research, a reliable stage measurement.

KEYWORDS

flood, flood monitoring, FFT, river sound, river stage, sonohydrograph, Storm Ciara, Storm Dennis

1 | INTRODUCTION

Hydrometry—the measuring of components of the hydrological system such as river flow characteristics—is crucial in flood mitigation strategy and monitoring (Chacon-Hurtado et al., 2017). The methods by which rivers are monitored are ever evolving with new techniques such as particle image velocimetry (PIV) and acoustic Doppler current

profiling (ADCP) measuring flow velocity, and ultrasonic depth meters (UDM) measuring stage (Kruger et al., 2016; Muste et al., 2004, 2008). There is a drive for greater ease of use of this kind of technology, being spurred on by the Internet of things approach (IoT) to create an easy-to-use framework that everyone can contribute to (Moreno et al., 2019). These approaches are designed to supplement the 1500 hydrometric stations currently operational in the UK (Marsh

This is an open access article under the terms of the Creative Commons Attribution License, which permits use, distribution and reproduction in any medium, provided the original work is properly cited.

© 2021 The Authors. Earth Surface Processes and Landforms published by John Wiley & Sons Ltd.

and Hannaford, 2008). Although the UK network of government agency hydrometric stations is dense, this equates to one monitor per 130 km of the river network (Marsh, 2002). All of these technologies, both existing and emerging, have infrastructural issues to overcome to work efficiently, such as power, direct line of sight and calibration, limiting their wider implementation. There is a need for an innovative, non-invasive, cost-effective method for monitoring river stage, which could be distributed throughout parts of catchments that currently are not monitored. Imagine being beside a river, what do you hear? In this study we propose that sound can be used as an alternative method to calculate river stage and track flood peaks. The use of sound is based upon the assumption that a river gets louder as its depth increases, such as a babbling brook becoming a thunderous torrent, generating a soundscape that is dependent on river condition. We focus on sound because it has a number of potential advantages over alternative methods for measuring river stage. Measuring sound is power efficient as the monitor measures passively, rather than actively generating a signal, such as an ultrasonic pulse from a UDM. PIV requires illumination at night, which can be a significant drain on energy. Sound can be measured from the banks of a river, reducing the need for extensive in-stream infrastructure. Despite its potential advantages, we do not currently know under what range of conditions sound can be used to monitor river stage. A method that works across a wide range of conditions is necessary for this technique to be used to manage flood risk.

The sound of a river has been studied through the use of seismic (ground), infrasonic (air) and hydroacoustic (water) surveying, examining how sound production can be linked to sediment transport, flood processes and turbulence within a natural environment (Manasseh et al., 2006; Ronan et al., 2017; Schmandt et al., 2017). The sub-aerial sound of a river is primarily produced by the entrainment and collapse of air bubbles in the flow, through turbulent features such as hydraulic jumps, rapids or waterfalls generating waves and whitewater (Bolghasi et al., 2017). Minnaert (1933) first described how the sound of 'musical' air bubbles and running water were complex in nature. The Minnaert resonance is the idealised sound frequency at which a bubble bursts, without the effects of surface tension, viscosity of the liquid and the thermal conductivity of the gas (Gaunaurd and Überall, 1981). Bubbles monitored underwater were found to burst in the frequency range of 400–2000 Hz, with bubble radius determining the frequency (Chicharro and Vazquez, 2014). The larger the bubble, the lower its corresponding frequency; for example, a 10 cm bubble radius has a frequency of 32 Hz and a 1 cm radius of 326 Hz (Leighton, 1994). We expect that this frequency range will determine the frequencies in the sound made by rivers sub-aerially.

The relationship between sub-aerial sound and stage level has been investigated by Morse et al. (2007). They concluded that as stage changes then sound pressure, the deviation of air pressure from ambient, will change in unison. The presence of geomorphic features, such as a cascade or riffle, were found to affect the sound pressure ranges. The study, however, had limited observations, with six to eight sound points over a range of flow conditions that did not include flooding; nor were the mechanics of what controlled the sound considered. The extrapolation of a relationship found during low flow to high flow has not been tested, with high flows having an inherently different flow regime, with surface turbulence structures emerging (Chanson, 1996). A relationship between seismic noise, sediment

transport and river discharge was found by Govi et al. (1993) and Anthony et al. (2018) and with river stage by Burtin et al. (2008), determining that hydrodynamics were the most probable source of the signal. Infrasound monitoring by Schmandt et al. (2013) suggests that waves on the water surface generated sound, showing a link between discharge and sound. The use of passive sound above the water is also seen as an emerging way of measuring the air–water gas exchange velocity (K), which is essential for ecological processes (Klaus et al., 2019; Morse et al., 2007). Klaus et al. (2019) found that there was a positive relationship between sound pressure and K in the frequency range 31.5–1000 Hz. The riverbed morphology had a significant control over the sound produced by each reach, with large-scale roughness elements (RE), such as boulders, having a larger effect than a gravel bed. A large obstacle will also cause the most deflection of the water, called form drag, at low and high flow (Bathurst, 2002). Looking at the self-aeration process, the mixing of gases from the atmosphere into the water, Kucukali and Cokgor (2008) found that there was a relationship between the blockage ratio (upstream area blocked by an obstacle) and aeration caused by turbulence. With a relationship between the size of an RE and turbulence, this supports the idea that REs are important to sound generation. We therefore seek to expand our understanding about a link between sound and REs and whether this has any influence on sound and stage relationships. The aims of this paper are to: (1) identify sites suitable for sound monitoring; (2) determine if river sound can be isolated from a complex, seasonal soundscape, outwith clement conditions; (3) investigate how factors such as REs may influence a relationship between sound and stage.

2 | METHODS

We first introduce our process for determining site suitability and the techniques to record and analyse sound data from rivers. We then examine the relationship between the recorded sound and river stage, and explore the factors that contribute to the relationship.

2.1 | Sound collection

All audio from our field locations (introduced below) was recorded in the WAV format at 16 kbps, as it preserves more data in a recording compared to a compressed format such as MP3. Mennitt and Frstrup (2012) used consumer-level recorders for outdoor audio recording and found that although MP3 allowed long, continuous recordings to be made, it did reduce the frequency resolution that could be used. Recording at a sampling rate of 44.1 kHz, with a Nyquist frequency of 22.05 kHz, the recording captures all data in the frequency range between 1 and 22.05 kHz, which is greater than the range of normal human hearing of 20–20 kHz (Horii et al., 2018). However, because of limitations in the response of consumer-grade microphones to low-frequency sound (Table 1) and due to power-source noise, we only consider frequencies >50 Hz in this study. We define river sound as the sound that can be audibly heard by a person, since we expect that someone can audibly tell the difference between a river at low and high flow. Infrasound, below 20 Hz, is not considered as consumer microphone frequency ranges rarely go below

20 Hz and, with the range at which humans can hear, a change of rivers sound is audibly noticeable. Bubbles would also need to be bigger, at greater than 30 cm diameter, to produce sound below 20 Hz (Leighton, 1994).

In this study, three types of microphone are used, with their technical specification shown in Table 1. Although less than ideal to use different microphones, once converted into sound pressure level (SPL), our sound value is measured in decibels of SPL (dB SPL) in reference to 20 μ Pa. Understanding how the sound changes is more relevant to our study and not why one river is louder than another, since other factors such as sound attenuation would need to be accounted for for direct comparison. All microphones were recessed within an enclosure to protect against wind and rain, but not blocked to the environment.

2.2 | Site suitability

In order to identify the most suitable sites we need to know how the sound produced by a river channel changes spatially and what river features influence it. We deem a site suitable if (1) we can hear the river and (2) if there is a significant response in the sound between river stages. We addressed this at the River Washburn, Yorkshire, UK, where there was a unique opportunity to record audio in the same day during a low compensation discharge of 0.08 $\text{m}^3 \text{s}^{-1}$ and a high continuous discharge of 8.55 $\text{m}^3 \text{s}^{-1}$. The Washburn is a natural river channel connecting a series of reservoirs, and occasional high discharges move water between the reservoirs. These releases are used for whitewater sports, and the channel has been managed by introducing rapids and boulder gardens (REs), altering it from what it would have been naturally.

To investigate site suitability an acoustic map along 500 m of the river was generated to help us identify regions that had a markable change in sound from low to high flow. Markers were placed at 10 m intervals along the course of the river, and each point was referenced using a dGPS. Recordings were taken at an elevation of 1.5 m above the bank during high and low conditions from the marked location. An additional section of the river was identified for a more in-depth examination, which had a flat floodplain around an RE to examine how sound behaves at different monitoring points around a channel. Mapping the sound at 10 m intervals along the river, and at 1 m points away from the river, we are able to describe how sound behaves. Audio was recorded for 8 s at each location, using the RØDE VideoMic (supercardioid) with a sensitivity azimuth of 210°, which is more directional in comparison to omnidirectional microphones at

360°. We used a supercardioid microphone to record the majority of sound produced by each specific section of the channel, and to limit sound from sections further up/downstream. However, components of upstream and downstream will still remain.

Photographs of each marker section were taken to assess what was generating the whitewater at each reach and to designate if a section had: no REs (Rank 1), small REs (Rank 2) or large REs (Rank 3). Qualitative ranking of the REs is used as direct measurements of these obstacles was not possible. Determining rank was done by eye, with ranks 2 and 3 differentiated by whether there was a large RE (height approximately >1 m) and how the REs were dispersed, such as how directly in the flow they were. It was assumed that an RE in the middle of the flow will have more impact on the flow than at either bank side.

2.3 | Sound analysis

With the sound captured, we needed to find a way to filter any noise from our expected river signal. Audio clips were converted from the time to frequency domain using a fast Fourier transform algorithm (FFT) in MATLAB R2020a. To examine at a resolution of 1 Hz, a minimum sample length of 1 s is required.

We aim to identify a river sound zone (RSZ), which is the frequency range that best correlates with river stage. To derive a single sound value for each recording, which can be compared against the corresponding river stage measurement, we use the spectral centre (median) of the data. The median is calculated from all values of SPL within a certain frequency range, known as a bin. As the FFT produces an SPL value for every 1 Hz, we have 22,050 individual sound values, with 0 Hz being the mean of the data. Therefore, when we calculate a median from a 1 kHz bin, it is calculated from 1000 values. We use this instead of the spectral centroid (average) or maximum volume, because the median of the data yields a more representative signal that is not skewed by erroneously large or low values in the frequency range. Median filters are useful in scenarios where periodic patterns are found (Ohki et al., 1995). The first bin of 1–1000 Hz is clipped to 50–1000 Hz, as due to the switching power supply used, noise from the power supply affects readings below 50 Hz.

It is unrealistic to assume that the only sound source is the river. To further constrain the RSZ, other environmental noise needs to be removed. Certain frequency domains that may be of influence are: the human voice in mainly the 100 Hz – 8 kHz range; birdsong at 1–8 kHz; and vehicles at 0–4 kHz (Liu et al., 2013; Monson et al., 2014; Slabbekoorn & Ripmeester, 2008). These noises will primarily affect

TABLE 1 The monitors and their associated microphones units within them

Monitor	Microphone	Directionality	Frequency range	Signal-to-noise ratio (dBA)	Sensitivity (dB) (1 kHz at 94 dB, 1 Pa)
River Washburn	RØDE VideoMic	Supercardioid (rejects 150° to rear)	40 Hz – 20 kHz	79	–38
Bushnell E3	ECM-60C	Omni	50 Hz – 13 kHz	40	–64
Raspberry Pi	CMA-4544PF-W	Omni	20 Hz – 20 kHz	60	–44

Note: Technical specification of the microphones is freely available online. Values that are important to the study are frequency range, signal-to-noise ratio and sensitivity. These determine the range we can measure at and also the conversion into sound pressure level. Each microphone has a quasi flat response to frequency as per the technical specifications but was not tested in this study. Any frequency bias will have a negligible effect on our data.

monitoring during low flow conditions, as during high conditions these will either be absent or drowned out. Figure 1 shows the spectrogram of each of these individual noises. Each sound has its own unique fingerprint, compared to a pure river signal. Birdsong has excitable chirps and trills, car sound is a wideband, flat noise, and talking is in pulses of speech. To reduce the number of noise-related errors, the RSZ will have to be both strongly linked to the river while maintaining its independence from these other environmental noises.

Wind and rain are not associated with a certain frequency range, and are dependent on intensity instead. Because of the fluctuating nature of wind and rain intensity, this rumbling, roaring sound is known as Brownian noise (Yackinous, 2015). Rain was found by Burtin et al. (2011) to have caused a seismic signal when landing on rocky debris near monitors. Wind can be the most intrusive sound on a recording and, if the wind is constantly louder than the river, blowing out the microphone, then it is not possible to extract a river component. In a remote location away from cultural noise sources, wind

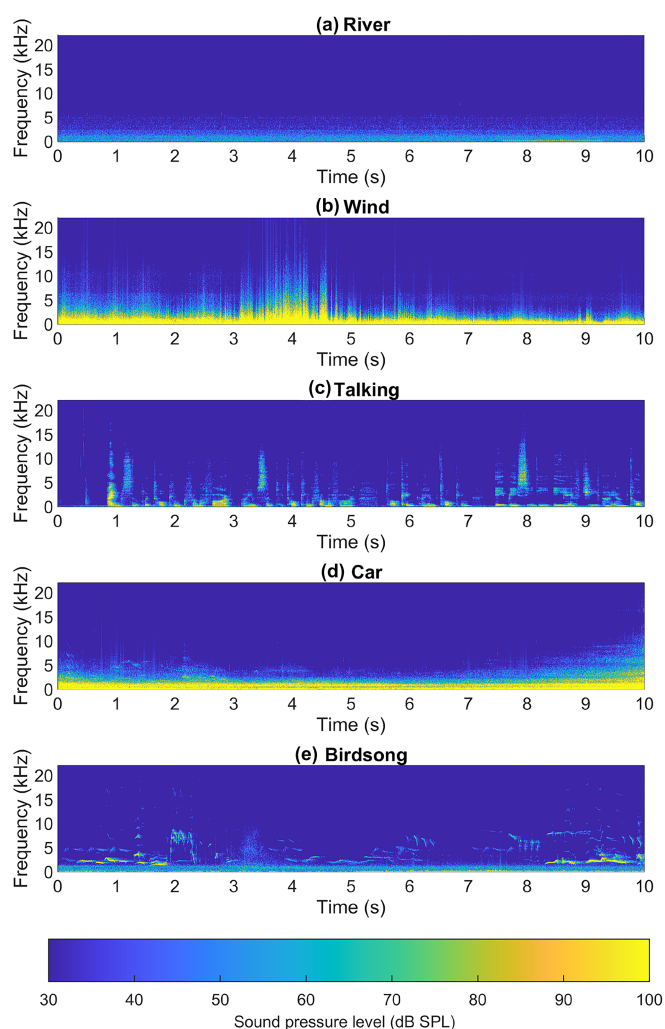


FIGURE 1 Spectrograms for different sources of environmental noise. Each recording is only of that sound: (a) Chainley Burn during average flow condition on a calm day; (b) Trout Beck, County Durham, during continuous high wind; (c) reciting the alphabet; (d) main road with cars going past; and (e) blackbird. Plots are produced by the spectrogram function using short-time Fourier transforms, which allows both frequency and time domain to be viewed concurrently. Bin width is set to 1 Hz to show a finer resolution of data [Color figure can be viewed at wileyonlinelibrary.com]

has also been recorded on seismic monitors at the surface, contaminating the recorded signal at speeds of only 6.5 mph (Withers et al., 1996). Ronan et al. (2017) found wind to be the most probable source of high power, low spectral coherence noise on infrasound recordings, while Anthony et al. (2018) suggested that without wind filters, and if deployed close to a river, infrasound acoustic signals were likely unsuitable for smaller river systems. To reduce wind impact on the monitor, the microphone can be placed in the opposite direction to the prevailing wind or placed in an area with adequate wind baffling from trees or shrubs. But, even with adequate protection, wind can still be heard in some recordings. Figure 1b shows the spectrogram of a gusty signal, with the bright peaks caused by intermittent wind spreading into the higher frequencies. If the entire recording was run through the FFT code, then these peaks spanning the entire frequency range would dominate the results.

To remove the impact of the wind we apply an additional filtering step to our data (Figure 2). We record each sample for as long as possible, as it provides a better chance of getting a continuous section of recording without wind noise. Changing the recording length is subject to the site and how confident we are that we can filter out the wind physically. In this study we considered a minimum recording length of 5 s to be necessary. To filter out the wind noise, we split the recording into 1 s rectangular windows, with a 0.5 s overlap between them. We do this to allow a frequency resolution of 1 Hz to be maintained through the FFT, as this matches our sampling rate. A rectangular window also does not smooth out the boundaries of the clip. Reducing the total recording length reduces the number of windows and thus the potential samples to get the lowest median from. The overlap is to increase the number of windows that can be taken from any given recording. The audio data from each of these new windows are processed with the same FFT code, resulting in one median value per frequency bin for each window. The minimum value for the RSZ, the region of frequencies found to have the maximum correlation with stage, from across all the different time windows is chosen. We take the minimum value from all the different time intervals because it is expected that river sound is constant in any recording and will always be the loudest of any constant base sound but will also be quieter than sporadic noises caused by wind, thunder, etc. By taking the minima of each audio sample in the RSZ, we can significantly improve the processing of noisy recordings. We call this the lowest median filtering (LMF). When assessing this technique to determine any bias in the window that is chosen, we found that the window with the lowest value is equally taken from across all the windows and one is not preferentially choosing one.

The following section introduces our workflow of collecting and processing river data, which was applied to all study sites and is the basis for any future work or different sites (Figure 2).

2.4 | Study site monitoring

Six sites were selected for monitoring between November 2019 and February 2020, based upon the findings of data collected at the River Washburn for site suitability, chiefly the occurrence of REs (see Figure 3 and Table 2 for characteristics). These locations were selected to be typical of many rivers and not highly specific. Sites a–c were deemed to have good site suitability. Sites d–f were not

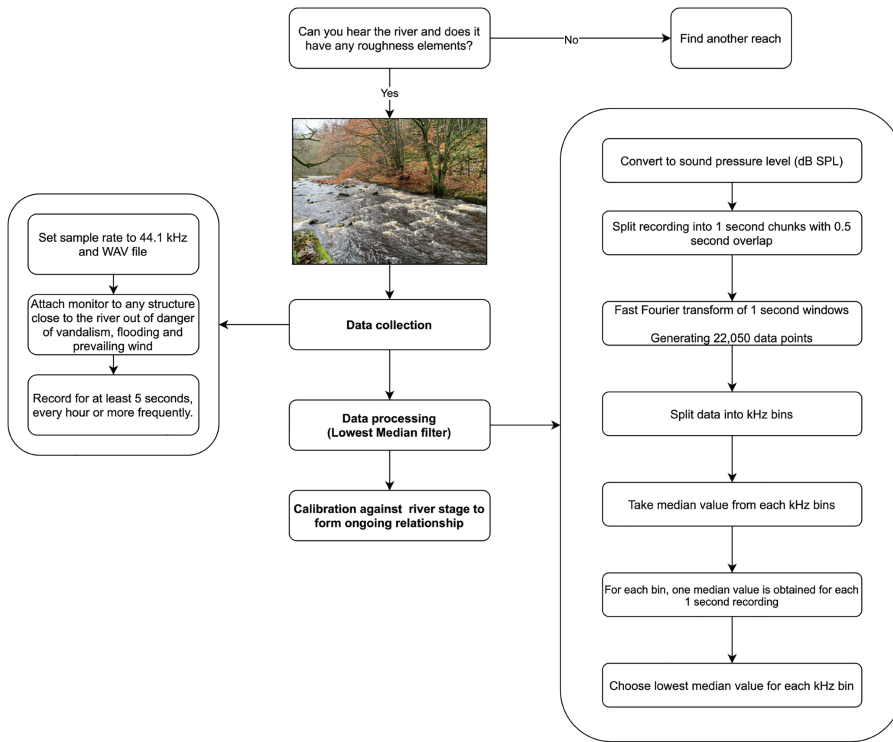


FIGURE 2 Our workflow of how to monitor a river using sound with the required steps needed to perform lowest median filtering [Color figure can be viewed at wileyonlinelibrary.com]

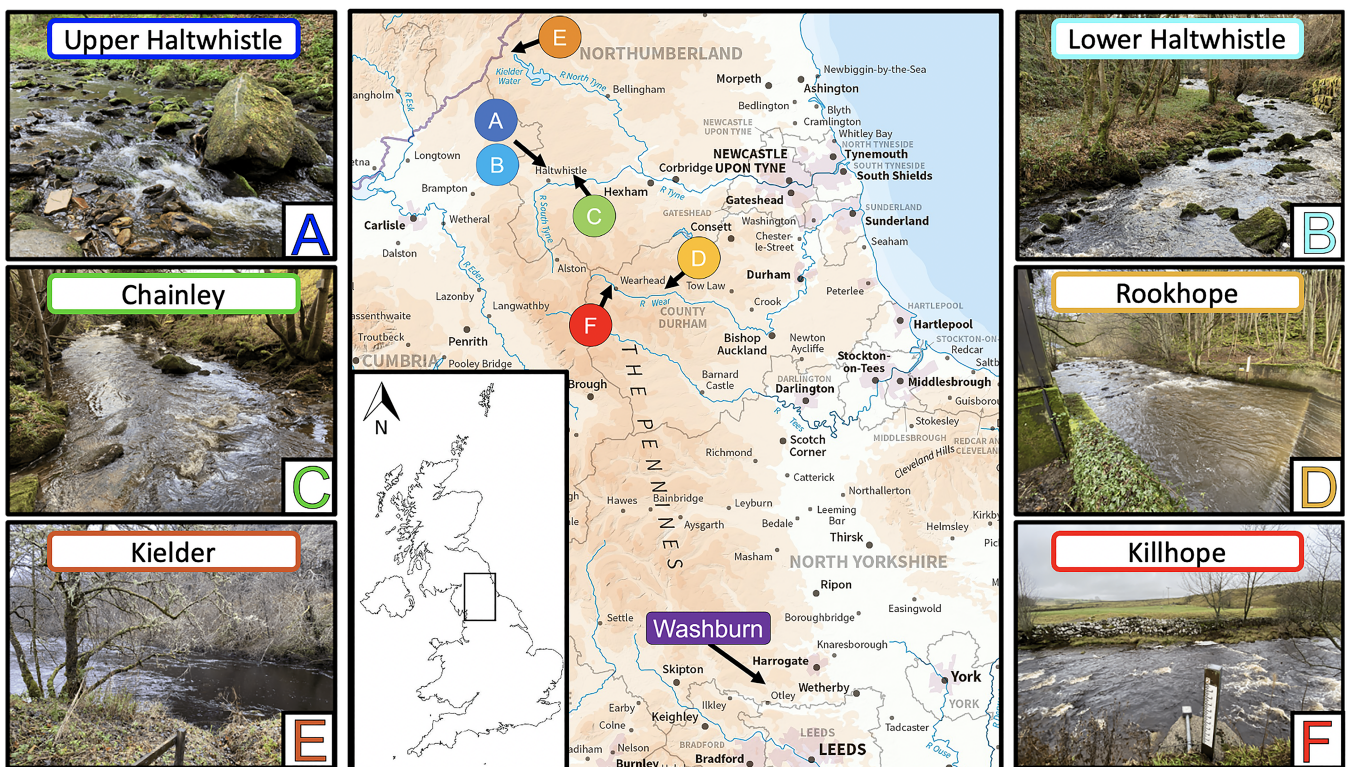


FIGURE 3 Map of study site locations with corresponding photographs taken from each site, showing the morphology of the river and the general surroundings. a–d were taken during low river levels, with e–f taken during above-normal levels. Approximate channel widths: A, 6.0 m; B, 6.0 m; C, 5.0 m; D, 8.0 m; E, 13.5 m; and F, 5.0 m [Color figure can be viewed at wileyonlinelibrary.com]

explicitly chosen for good suitability; for instance, many have small REs and Site F has a large amount of wind noise. They are predominantly alluvial rivers but include two bedrock channels (Sites D and F), and range between 8.0 and 34.5 m wide. Stage at Sites A–C was measured using a pressure transducer (TD-Diver), calibrated to atmospheric pressure, and Sites D–F were Environment Agency operated gauges recording at 15 min intervals.

A Bushnell E3 trail camera was used to record sound at Site A as this provided a ‘ready to go’ set-up at the start of the project. A purpose-built monitor was created from a Raspberry Pi Zero, a CMA-4544PF-W microphone and a WittyPi Mini (timer) for use at all subsequent sites. Monitors were attached as close as possible to the river on existing structures and out of danger of high water. At Site A sound was recorded for up to 10 s, once an hour due to running off of

TABLE 2 Study site location properties

Site	River	Coordinates	Data collection period	Gauging	Distance from monitor to river bank (m)	Bankfull depth (m)	Bankfull width (m)	Substrate
A	Haltwhistle Burn (Lower), Northumberland	54°58' 43.5" N, 2°27' 40.6" W	24/07/2019 – 19/02/2020	Diver	1.0	1.6	14.3	Cobble
B	Haltwhistle Burn (Upper), Northumberland	54°58' 47.2" N, 2°27' 36.4" W	28/01/2020 – 19/02/2020	Diver	5.0	1.1	19.9	Cobble
C	Chainley Burn, Northumberland	54°58' 51.1" N, 2°21' 22.7" W	6/12/2020 – 19/02/2020	Diver	1.5	1.4	9.8	Cobble
D	Rookhope Burn, County Durham	54°44' 51.0" N, 2°04' 31.0" W	27/11/2019 – 14/02/2020	EA	4.5	0.8	8.0	Cobble/Bedrock
E	Kielder Burn, Northumberland	55°13' 50.9" N, 2°34' 54.0" W	27/11/2019 – 16/02/2020	EA	13.0	1.5	34.5	Gravel
F	Killhope Burn, County Durham	54°45' 11.7" N, 2°13' 27.5" W	27/11/2019 – 18/02/2020	EA	7.5	0.8	8.7	Bedrock

AA batteries. A reading once an hour is the minimum frequency to monitor at, as anything longer than this becomes uncondusive for meaningful flood monitoring. Higher frequency sampling rates of every 15 min were achieved with the Pi Zero at Sites B–F, allowing comparison against the 15 min interval EA station data. Each device has a finite number of recordings it can take, due to the size of battery used, meaning it can either sample at a high rate for a short time, or last longer and only sample every hour. Using a 7 Ah, 12 V lead acid battery allowed up to 1400 recordings to be made with the Pi. The length of individual recordings varied due to power saving management, with the wildlife camera varying between 8 and 10 s and the Pi Zero 9–10 s.

With the exception of the acoustic mapping, an omnidirectional microphone was used in the monitors as this captures audio from an identified reach, without the need to target the microphone during installation. There would be a risk of a supercardioid microphone moving during any long-term experiment, which would incur an extra source of error. The ambition to make a sensor that can be widely deployed means that it is advantageous if it can use cost-effective and easily procured components. Higher resolution and frequency response data could be captured with a higher specification microphone and digital audio recorder, but with the problems of power and cost becoming an issue. We expect that the frequencies that will be of interest are less than 15 kHz, so the microphones used should be sufficient (Klaus et al., 2019).

During our monitoring, the UK was subjected to substantial rainfall in February 2020, with Storm Ciara on 8–9 February, and Storm Dennis on 15–16 February. These events produced river levels that reached the highest levels monitored in some of our stations, and higher than levels reached from Storm Desmond (5–6 December 2015) for others but not quite beating long-standing records. Having both storms back to back was an incredibly rare opportunity. We use the data from the storms as our primary dataset, because it ranges from very low to very high levels, and therefore can be used to test the range of conditions across which sound can be used to predict stage. We supplement this data with a longer dataset collected at Site A from 24 July 2019 to 20 February 2020.

3 | RESULTS

We present our results in three stages: (1) analysing what features within a river may control the sound emitted and determine a suitable site; (2) demonstrating how the LMF helps to improve the data collected from the river; and (3) examining whether the filtered sound data have any correlation to river stage.

3.1 | Acoustic mapping

3.1.1 | River Washburn

An acoustic map of the River Washburn is shown in Figure 4 during low and near bankfull flow. The River Washburn has an SPL of 30–60 dB SPL across its course during low conditions, with higher values at a weir and a constrained section. At high discharge certain reaches

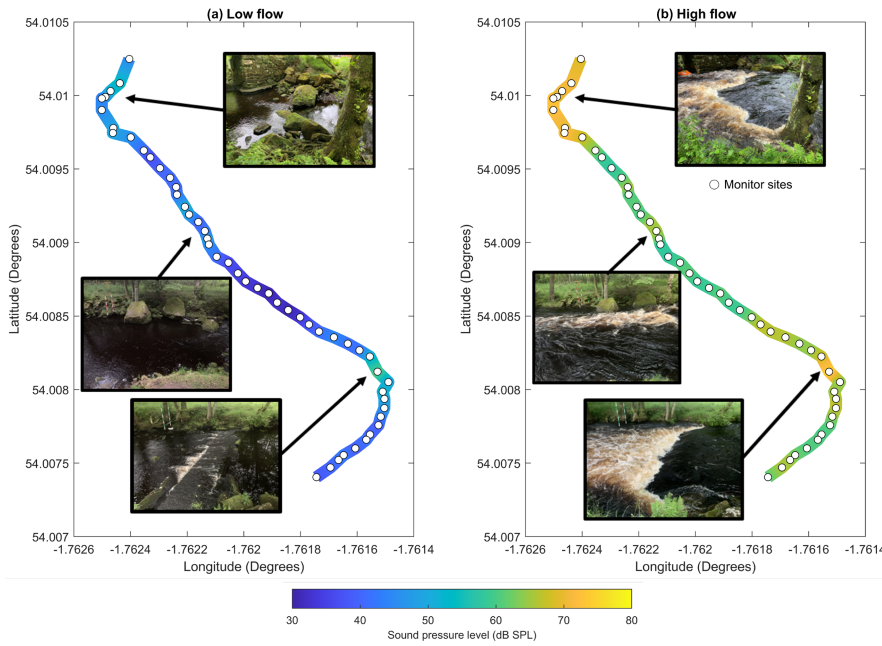


FIGURE 4 Acoustic map plotted of a 500 m course of the River Washburn during low and high flow. Markers show recording locations, with the coloured line being a 1D interpretation between these points. Images shown highlight the main areas of change along with photographs of the sites. Sound values are obtained using the lowest median filter with a frequency of 0.05–1 kHz. This range is used due to the site being sheltered from wind, meaning that any sound generated will be purely from the river [Color figure can be viewed at wileyonlinelibrary.com]

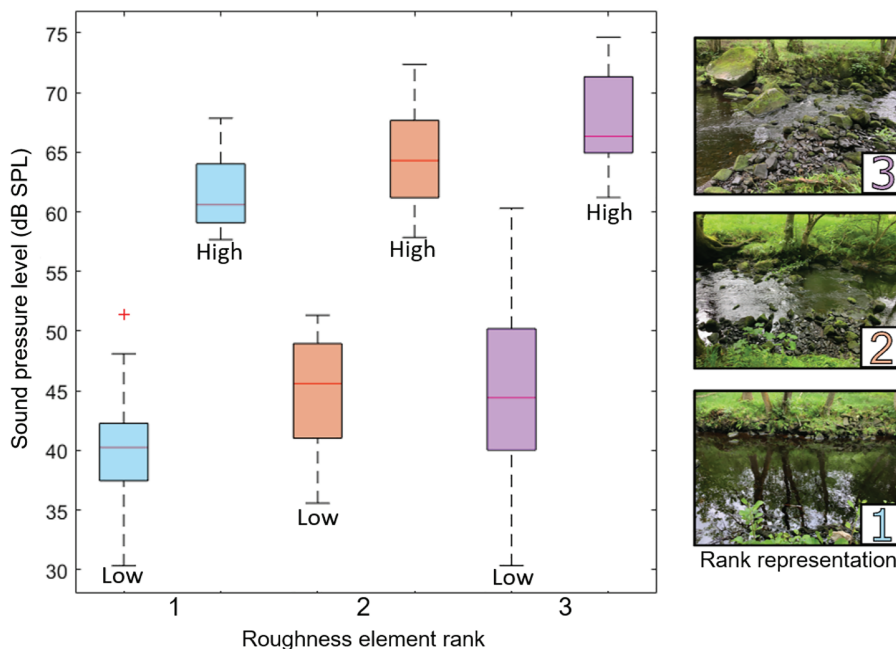


FIGURE 5 Box plot of normalised amplitude at low and high flow conditions, grouped by the qualitative rankings of roughness elements at the River Washburn. Photographs show a representative example of each rank. Roughness element rank is chosen by eye, with dominant REs—that is, the largest element—being easily identifiable in Rank 3. Number of samples: Rank 1, 22; Rank 2, 15; and Rank 3, 13 [Color figure can be viewed at wileyonlinelibrary.com]

become very loud, where there are substantial REs with heights >0.5 m. When observing the photographs at each section, we found a correlation between the presence of whitewater and the SPL, with more whitewater being associated with higher SPL values, agreeing with (Ronan et al., 2017). Every section of the river experienced a rise in SPL from low to almost bankfull flow. When comparing to the qualitative RE rankings in the channel: Rank 1 generates a median range of SPL between 40 and 60 dB SPL; Rank 2, 46–64 dB SPL; and Rank 3, 45–66 dB SPL (Figure 5). Therefore, between low and high flow, SPL rises by around 20 dB SPL no matter what rank is used. However, choosing the rank in which the loudest sound is produced is beneficial as it provides a higher likelihood of being louder than any possible environmental noise.

An in-depth look at a section of the river with a large RE, with a rank of 2, is shown in Figure 6. In Figure 6a, as we walk 10 m away from the river, the SPL drops from 66 to 55 dB SPL during high flow.

At every point, the SPL measured at high flow is larger than that measured at low flow. Moving upstream or downstream, Figure 6b shows that SPL drops as we move away from the RE. The highest SPL is not at the RE as a tree was between the microphone and the RE. Without the tree we would expect a smooth convex shape to continue. Sound does not drop as much as when moving away from the river, with a 10 m movement causing a drop from 66 to 61 dB SPL.

3.2 | Lowest median filter

3.2.1 | River sound–stage relationship

Long-term audio data, recorded using the trail camera at Site A, are compared against the river stage data from the pressure transducer in Figure 7. The audio data were processed to calculate the median SPL

FIGURE 6 At the River Washburn, acoustic mapping was done around a dominant RE with a rank of 2: (a) moving away from the river and (b) along it. Recordings were done at the same points during low and high flow. Sound value relates to the 0.05–1 kHz band after lowest median filtering [Color figure can be viewed at wileyonlinelibrary.com]

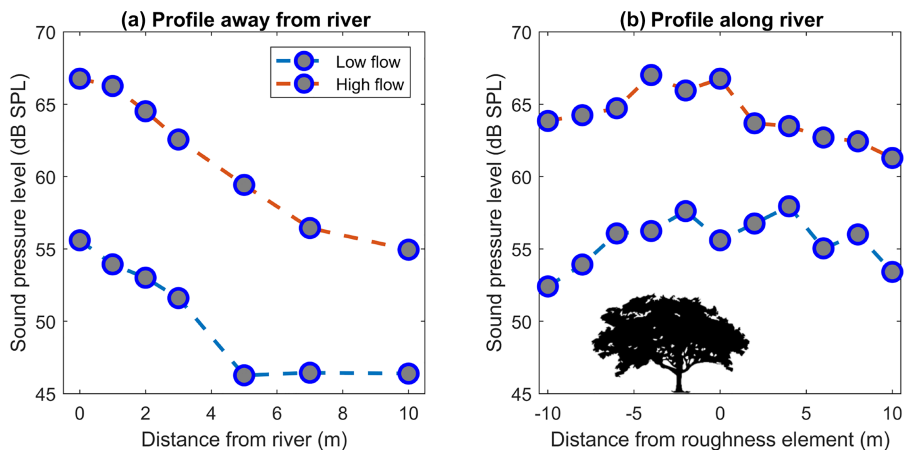
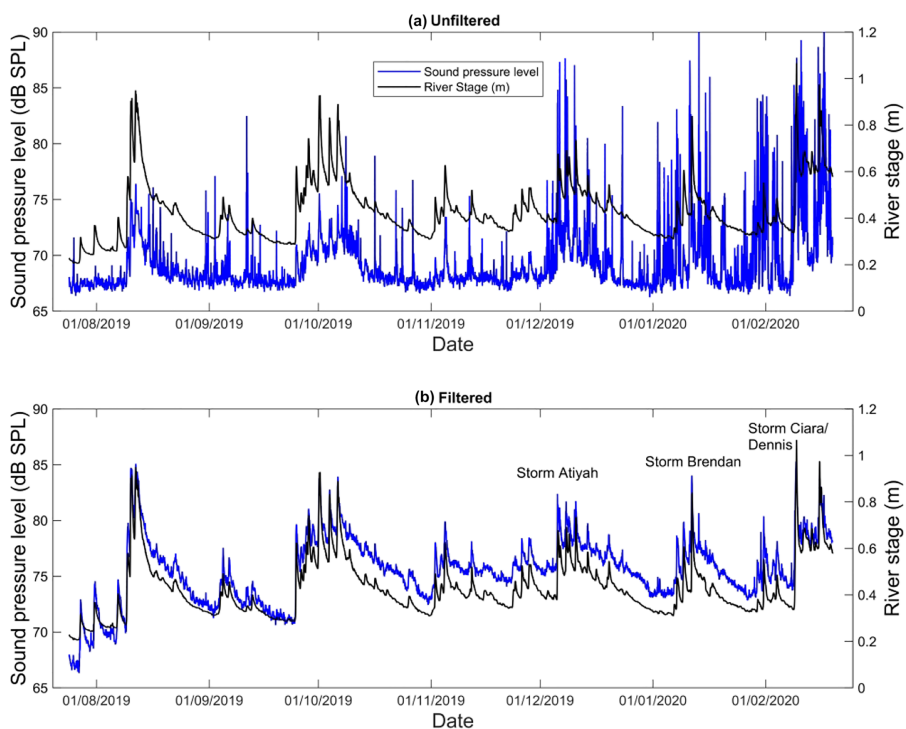


FIGURE 7 Sonohydrographs (blue) and hydrographs (black) of the Haltwhistle Burn over a summer/winter season. (a) Unfiltered data at 0.05–1 kHz and (b) LMF filtered data at 0.05–1 kHz. Unfiltered data are an FFT of the entire audio clip, and the median taken from the 0.05–1 kHz bin [Color figure can be viewed at wileyonlinelibrary.com]



within the frequency range 0.05–1 kHz. The frequency range was chosen to illustrate how well the filter works, although it may not be the best frequency range to use in the study due to the prevalence of wind. We call the resulting profiles of how sound changes over time sonohydrographs. In Figure 7a there is little similarity between the sonohydrograph and the actual hydrograph. In contrast, in Figure 7b after LMF the sonohydrograph has the same shape as the hydrograph, with the steep sides of the rising limbs and the slower lowering of the falling limbs. In Figure 7a the wind noise produced by winter storms is clearly highlighted in the large fluctuations of the blue line such as on 9 February 2020, with no clear signal being given during this time period. If used to interpret river stage, the river would appear to be in a state of flooding and sudden drainage repeatedly. In contrast, in the filtered data, there are no fluctuations. We therefore apply the LMF in all subsequent data analyses.

3.2.2 | Wind noise

The Killhope Burn, at Site F, is a far noisier site in comparison to the more secluded locations such as Haltwhistle, with traffic and wind noise (Figure 8). As shown in Figure 1, these pollutants share the same frequency space as the river sound, meaning that we needed to use a higher frequency range of 5–6 kHz, as it was shown later in the study to be the best to use at this site. The readings are affected by wind even during periods of more settled weather, with Storm Atiyah, 8–9 December 2019. The filtering has an enhanced effect compared to Figure 7, removing most of the fluctuating readings and reducing the scatter of the data. We still have some wind noise artefacts in the data in Figure 8c, but significantly less than in Figure 8a. The number of points in the data where the SPL is an order of magnitude greater than the value of the previous point is reduced by 70% after

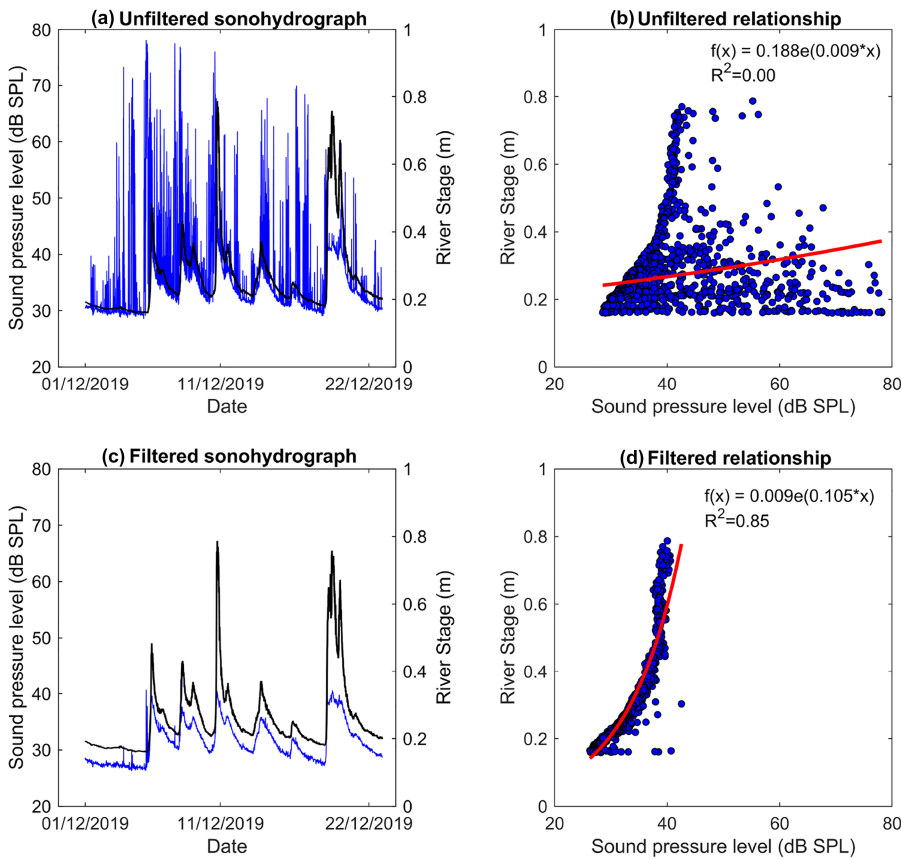


FIGURE 8 Comparison of river data with substantial wind noise from the Killhope Burn, Wearhead, between 5 and 6 kHz. (a) Unfiltered sonohydrograph; (b) unfiltered river stage–sound relationship; (c) LMF sonohydrograph; and (d) LMF river stage–sound relationship [Color figure can be viewed at wileyonlinelibrary.com]

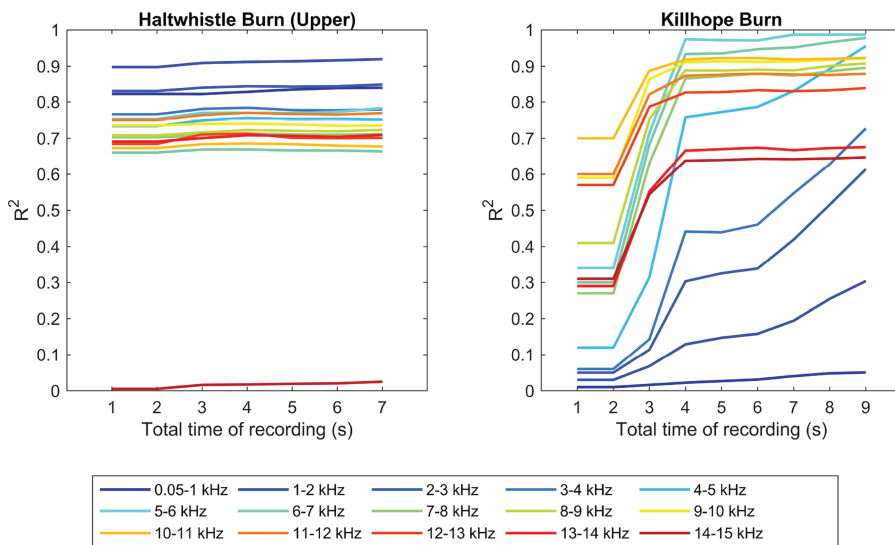


FIGURE 9 Sound data from Haltwhistle and Killhope filtered through the LMF using different total recording times and its affect on the stage–sound relationship R^2 value. Haltwhistle burn uses a logarithmic function to fit to the data, and Killhope uses an exponential function [Color figure can be viewed at wileyonlinelibrary.com]

application of the filter. The fit and smoothness of the sonohydrograph also improve when viewed in relation to river stage. When we plot river sound and its co-current river stage we are able to fit a function to this, with Figure 8b,d showing that an exponential relationship is able to be found, with an R^2 of 0.85 after the LMF, when before it was not possible. The wind noise that was persistent at low stages has all but been eradicated.

To allow the LMF to operate efficiently, a recording length has to be long enough to include a gap in any concurrent noise. We ran our LMF code with different lengths of recordings, from 1 s to total recording length. These new SPL values were then compared against

stage, and the R^2 found of the best relationship between the two. In Figure 9 the difference between the calmer Haltwhistle and the windier Killhope site becomes clear. Haltwhistle is able to achieve a better relationship against river stage at very short recording times, with a 1 s recording giving an R^2 of 0.90 in the 1–2 kHz bin. Conversely, a 1 s recording at Killhope only has an R^2 of 0.7. There is an upward trend in R^2 against recording time for both sites, but this trend is more substantial at Killhope. At a total recording time of greater than 2 s there is a substantial increase in R^2 in the Killhope data, with R^2 reaching 0.97. After 4 s there is a gradual increase of the fit. The filter is also improving the lower frequencies of the Killhope burn; however,

longer recording times would be needed to match the mid-frequencies. This demonstrates that the LMF is effective at reducing the impact of wind noise on our data.

3.3 | Storms Ciara and Dennis

Figure 10 represents February for the study sites located throughout the northeast of England. For each site we calculated the median

sound value after LMF filtering in bin widths of 1 kHz, plotted these values against river stage, and calculated an R^2 value of a logarithmic and exponential fit. Two fit options are used as some data fit better with an exponential compared to a logarithm. Our aim is to identify whether there is a relationship in the data, regardless of the form, rather than having a prior assumption about what the shape of the relationship should be. The variations in R^2 values with frequency range are shown in the first column of Figure 10. We use all the sound data during February (inclusive of storms) to determine the RSZ that

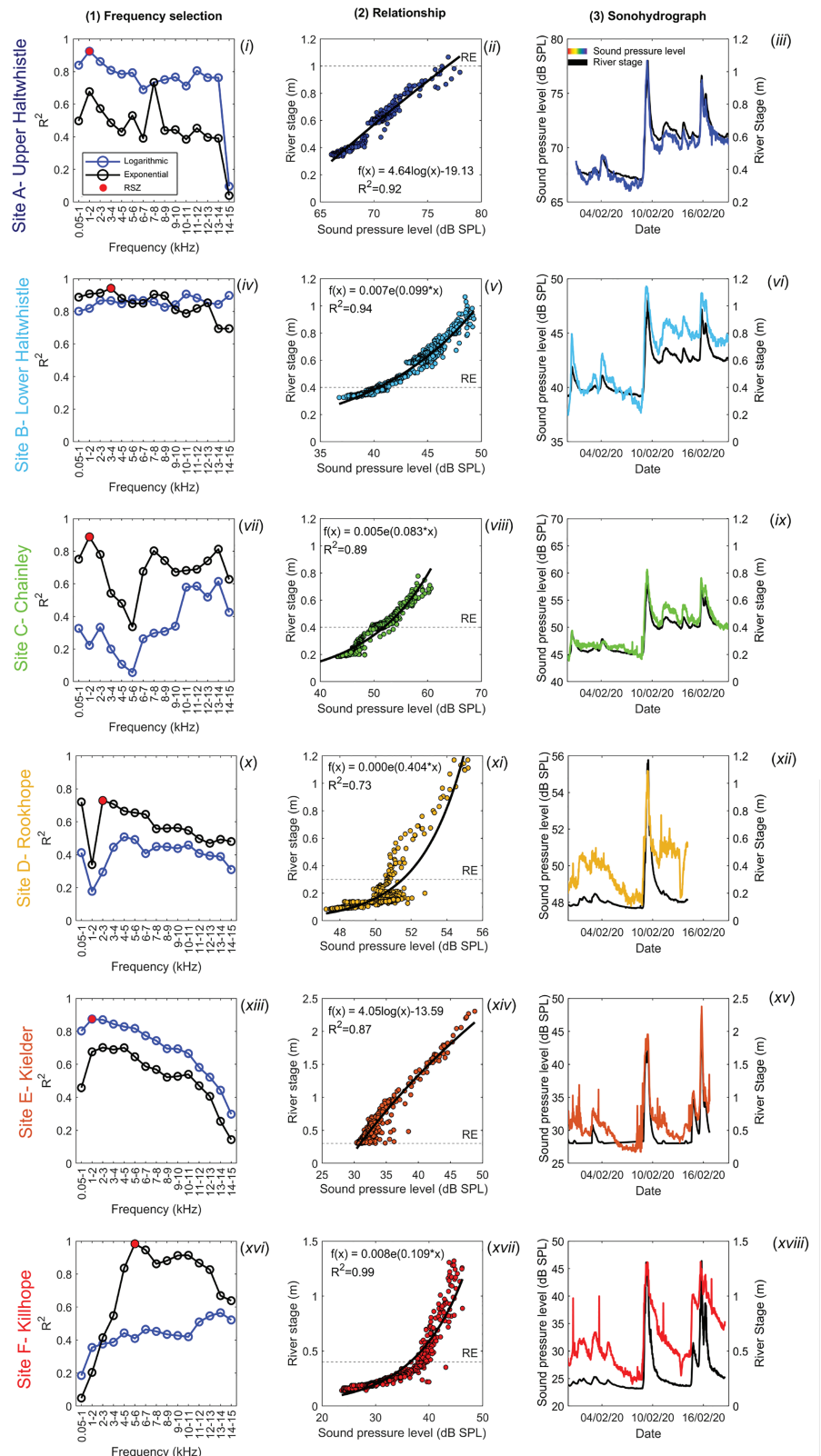


FIGURE 10 Workflow for identifying the best RSZ and obtaining the best river sound-stage relationship for our six sites during Storms Ciara and Dennis. Column 1: plotting of Storm Ciara/Dennis sound data against stage, forming an R^2 value for both a logarithmic and exponential function. Highlighted point is the chosen RSZ for the rest of the figure which is the highest R^2 value. Column 2: sound data and river stage plotted for the highlighted RSZ. Column 3: sonohydrograph and hydrograph comparison for the RSZ. Horizontal dashed line shows the highest point of the largest roughness element found in the channel [Color figure can be viewed at wileyonlinelibrary.com]

is most likely to be the best region to use going forward. Site D has relatively poor but consistent correlations throughout the spectrum between 0.05 and 15 kHz. We see that the highest R^2 values occur in the 0.05–3 kHz range in four out of the six rivers (Sites A, C, D and E). The RSZ used subsequently for each of these rivers is the highest R^2 found from fitting a relationship. Two sites have their best relationship with a logarithm, and four with an exponential. The R^2 values can vary across the frequency range in each river, with some being very consistent (Site B), to others being less consistent (Site C).

With the best RSZ determined, column 2 in Figure 10 compares the river stage data against the sound data recorded during February using the chosen bin (RSZ) highlighted in column 1. Each river shows a correlation between recorded sound and river stage, with certain reaches better than others. Sites A, B and C had very good site suitability and have been found to have among the highest and most consistent R^2 of between 0.89 and 0.94. In these sites stage modelled from sound is within 0.2 m of the actual stage at the 95% confidence interval. Sites D, E and F were not explicitly chosen for good site suitability but they do all still have a strong relationship, with R^2 of between 0.73 and 0.99. Data below 0.3 m at Site E have been removed since no comparable river stage data were available.

The highest river level was recorded at Site E, at 2.2 m. When the stage reaches 1 m, we see a large increase in SPL with subsequent increases in stage. Bankfull for this reach is at an average depth of 1.5 m, above which the river flows through riparian vegetation. At these levels any riverbed morphology will have been submerged, but other obstacles such as trees start to interact with the flow. Site E is the only site to have experienced significant above bankfull flow during this time period. Flow in other channels was kept within the banks by features such as built-up footpaths and flood defences. Site D was located at a weir/natural waterfall complex, with the shape of the graph perhaps reflecting this, with large variation of SPL below 0.25 m at 47–52 dB SPL. At low flow there may be two competing sound sources: the REs and the weir/waterfall. As river stage increases one sound source may become dominant, most likely the waterfall, and a less varied signal emerges.

Column 3 shows the hydrograph compared against the sonohydrograph. From the sonohydrographs we can see that there are a few peaks caused by wind, with some still found in Figure 10(xv, xviii). High gusts of 50 mph, and a sustained wind speed of 30 mph, in combination with low river level are the likely cause. The general shape between the two curves is the same during flooding. There is divergence between the graphs in Figure 10(xi) at lower river levels, before the peak emerging at 0.3 m. Site E does not record stage below 0.3 m; however, we have included our sound data in the sonohydrograph to show that we were still able to measure sound below 0.3 m.

4 | DISCUSSION

We have shown that sound shows a strong correlation with river stage after determining the best frequency range. Consequently, we think that it might be possible that, given reliable sound measurements and site calibration, a corresponding river stage can be estimated. Producing reliable estimations of river stage from sound requires consideration of how the river sound can be isolated from

ambient noise and how sound is produced by a river. Although this is preliminary work, it has shown promising results, albeit with requiring post processing at this stage.

4.1 | Controls on sound generation

In order to be able to implement monitors at different locations without the need for calibration, we need to be able to predict the form of the stage/SPL relationship. We expect that this will be a function of factors including the size of the largest obstacle, obstacle density, bankfull level, how close the monitor is to an RE, and whether there are any barriers between them that were shown to impact sound propagation (Figure 6). Our Washburn dataset leads us to the conclusion that for a site to be suitable for monitoring it is beneficial to have an RE within the channel since it produces the loudest sound. The variability in sound along the 500 m section is proposed to be entirely down to the RE presence, prominence or absence. The REs of these reaches impede the river, forcing flow around and/or over. The river has to exert its energy to overcome these, and some of this is released as sound energy from the entrapment of air and bursting of bubbles. When observing the photographs at each section (Figure 5), we found a correlation between the presence of whitewater and the SPL, with more whitewater being associated with higher SPL values. An entirely featureless reach, such as a culvert, would be less than ideal for this method, unless there was some sort of texture.

In our data we see upticks in the trend of the sound/stage data in Figure 10(viii, xi, xvii). The interruptions occur when an RE feature has either been submerged or perhaps when a new RE is activated. Site D, with its weir and waterfall, is an alluvial channel, with boulders of between 0.2 and 0.3 m. We believe that once the boulders have been submerged the loudest sound is generated from the waterfall complex, which at low levels is quieter than the boulder sound. Site F's RE is from stepping within the bedrock channel, with step heights of 0.35–0.45 m. Similarly with Site D, once these features are submerged, the trend seen in the data shows an exponential trend in sound being produced, with an increase from 0.5 to 1.4 m, having an SPL range of 40–45 dB SPL. The trend means that, as stage increases, the SPL will increase, but not at the same rate as during lower levels at the RE submergence height. The continued upward trend in data is hypothesised to still be originating from these RE, but from a different mechanism arising from the higher discharges. Turbulence structures created by the changes in flow may be generating different bubble structures for example, with fluctuations in intensity. Standing waves are the most likely cause of new turbulence at higher stages with submerged boulders, with localised increases in Froude number (Comiti & Lenzi, 2006). The preference of either an exponential or logarithmic function being fitted to the data is hypothesised to be linked to a self-limiting part of the system, with a river reaching a point that there are no other sound sources being activated. Sites with an exponential fit have their REs covered at low levels, and do not activate new ones even at above bankfull. Sites with logarithmic functions have either not had their REs covered or have broken their banks and activated new ones. To further test this hypothesis a river would have to be monitored at both in-bank and over-bank storm conditions.

In ranking the river reaches in Figure 5, sections without any REs still had an increase in SPL between low and high flow. We could

conclude that generally there is noise bleeding in from sections up/downstream, or that there are other sound-generating elements in a reach. Figure 6b has sound generated from an RE being observable 10 m upstream or downstream of it, which is within our 10 m sampling range. Therefore, the change in sound observed at a site with smaller REs (Rank 1) may in fact be affected by REs further away. The design of the river means that there were REs found throughout, and attributing a specific RE for bleeding is difficult. Bank resistance is another possible source of sound, such as from protruding tree roots or alluvial deposits. However, we expect that REs are the main sound source of sound within a river environment. Our Washburn data suggest that the larger the RE in the river, the greater the SPL at high conditions. Being louder is seen to be beneficial to monitoring, since the river is more likely to be louder than environmental noise and is broadcast over greater distances, meaning that monitors can be located further away. Rivers with smaller REs may still be able to be used, with the caveat of monitors perhaps needing to be more sheltered or closer to the river. In general, we can say that the larger the RE, the louder it can become, which therefore opens more flexibility in the monitoring regime. Assuming that large obstacles are near-permanent fixtures in the river, they remain stable even during high flow events. This stability should make any long-term data and future extrapolation of stage far easier than if the environment was constantly shifting. A moving obstacle would have the same effect as moving the microphone (Figure 6), changing the sounds that are monitored. Further long-term studies will need to be undertaken to determine how long a site's relationship remains stable; however, in Figure 7, over the course of 6 months the signal does not change drastically. Over this time, bedload will have been transported, but this movement did not change the signal we observed. In a more dynamic environment, a change in bed configuration may have a significant change in sound.

We can use the Storm Ciara data (Figure 10), where data were collected from channels with different REs, to determine whether an RE has any influence on a relationship. The data show that, regardless of RE size, a smooth relationship exists after RE submersion. However, the trend of that relationship appears to be ultimately controlled by the RE, such as in Figure 10(viii, xi, xvii). As all sites had REs, we cannot be sure if these sorts of relationships would still persist at sites without REs. We have shown that when using co-located measurements of sound and stage we can derive a relationship to predict stage to within 0.2 m at the 95% confidence interval. However, the ideal frequency band used to obtain stage information and the nature of the relationships are both highly site specific, so it is not currently feasible to predict the form of that relationship without some paired measurements of sound and stage. But, at all sites, SPL has increased with increasing stage. Consequently, the relative change in SPL of the river could be used, without calibration, to determine whether the peak of a flood has passed.

4.2 | RSZ isolation

When trying to determine the best frequency range to use in our research, we defined the best zone as the RSZ. We found the RSZ to change between different rivers within the range 0.05–6 kHz, with no set zone for all (Figure 10). The RSZ is influenced by how noisy the

signals fed into the LMF were. The greatest challenge faced by this study was the isolation of a river sound component from the ambient soundscape. Without the benefit of generating our own signal, we rely on the continuous burbling of a river, and if this primary sound source is obscured by other noises we need to actively search for a clean signal, which is why the RSZ is influenced. We expect that the main frequency range for sound production in rivers is in the lower frequencies, <3 kHz, as we experienced our most consistent R^2 values there, with one Site B having a marginally better R^2 at 3–4 kHz, but only by 0.03 compared to 2–3 kHz. We do still have very high R^2 values in higher frequencies, and a very good 0.99 for Site F. However, 0.05–3 kHz is heavily affected by wind noise, which if strong enough may require the switching to higher frequencies, as observed at Site F. Potentially, Site F may have had a strong relationship in the lower frequencies, but due to persistent wind noise we cannot identify it.

Research using hydrophones is consistent with our RSZ, with surface turbulence having a frequency range of between 500 and 2000 Hz over varying flow regimes (Geay et al., 2017). Tonolla et al. (2009) examined how relative submergence of an obstacle influenced the sound, stating that a frequency swap may occur once a relative submergence limit is passed, such as a riffle producing mid-frequency noise during low discharge, changing to a low frequency at high discharge. We do not see the complete abandonment of a frequency range after an RE is submerged, such as in Figure 10(xiv, xvii), as there is still a relationship with stage present beyond RE submergence. A frequency switch might be causing the change in direction of a relationship once an RE is submerged, but we cannot be certain on this since the low frequency needed to confirm this at our sites that display this behaviour is obscured by the wind. Other sources of sound produced from within a river, such as sediment transport, can exist in the same frequency space as turbulence, around 1 kHz (Krein et al., 2016). But we have not seen any indication from our data of sudden changes in our trends at high discharges. It might be that our rivers do not generate bedload sound loud enough to overcome the sound of turbulence, but in other rivers it might be a different case. The sound from sediment moving is not strongly transmissible through the water to the air, with acoustic pressure reducing by 2000 times when sound transfers between the two, meaning either there has to be a lot of bedload movement or for the turbulence sound to be lower than it for it to be heard (Leighton, 2012).

We use a frequency range instead of a single frequency to measure river level because, as river level increases, changes in the turbulence cause the bubble size to change, altering the frequency of the sound that is produced—the Minnaert resonance. Using a range also adds stability to the data. In the frequency range of 0.05–3 kHz, we are in the Goldilocks zone for sound production from surface turbulence, with filtering helping to remove any environmental noise. Within this range, each river has a different most efficient frequency to look at. But not all rivers have their best efficiency in this region, so the RSZ may need to be altered subject to analysis of previous data. We do, however, see that the sites chosen for good sound potential (Sites A and C) have RSZ in the 0.05–3 kHz region. The reason for better stage–sound relationships being found at higher frequencies when the lower frequencies are polluted, despite sound being produced in the 0–3 kHz region, is perhaps down to harmonics. If there is a fundamental frequency of 1.5 kHz, we can expect to see upper

harmonics at 3 kHz, 4.5 kHz, etc. reducing in SPL magnitude at each jump. Similarly, a range of fundamental frequencies may have these harmonics. Kumar and Brennen (1991) reported that the sound of bubbles bursting in water showed harmonics, with defined peaks occurring at higher frequencies above the fundamental frequency. It is perhaps with harmonics and overtones of the bubbles that we continue to see a river–sound relationship at higher frequencies.

Having identified that sound production is focused at <3 kHz, we need to ensure that we are able to monitor this region as easily as possible. The basics of sound isolation lie in the design and placement of the monitor. Eldwaik and Li (2018) noted that wind noise was notoriously difficult to filter in an outdoor environment, due to its time-varying nature and broadband frequency. We show that our LMF can help to reduce noise from the wind (Figure 8), but better still would be to not have the noise in the first place, achieved by having a microphone properly shielded from the wind. We recessed our microphones to protect them from the rain and wind, but still had wind noise present, meaning that without recessing our data may have been more affected. Adding a wind-dampening sponge could also be used, having the effect of quietening down the recording, but also baffling the wind (Lin et al., 2014). Even with these preventative measures, wind noise will still be present since it is part of the soundscape. With rivers that are found in exposed areas, however, such as moorland that are subject to frequent low-level wind, placement of the monitor becomes crucial. Placing a monitor as close to the river as possible has two benefits: the likelihood of hearing only the river, and also offering the highest range in sound, with a better resolution of data (Figure 6). We see that through acoustic mapping at the River Washburn, when the microphone is moved further away from the river, it begins to quieten. At every point, the SPL measured at high flow is larger than that measured at low flow. SPL decreases upstream and downstream of the RE, with the highest SPL near the RE. The decrease in SPL as you move up/downstream is less than that observed when heading away from the river, due to other sound components being introduced from the river. We do, however, acknowledge that placement beside a river is not always possible, and find that being within 5 m is advantageous, with the ability to move up to 10 m still having a difference between high and low (Figure 6). The limitation of how far a monitor can be placed is when the sound from high and low flow overlap, meaning that you can no longer monitor changes acoustically. The distance of how far a monitor can be placed is determined by the river itself; larger, more energetic rivers may be still within a zone of high relationship further than 5 m. Conversely, a smaller, less energetic river may need to have a closer monitor.

4.3 | Sound as a hydrometric

We are encouraged by the trends between sound and river stage we see in each river that we have monitored. Currently, we are able to model with certainty when river level is changing, with all sites in Figure 10 showing their flood peaks clearly from sound data. We acknowledge that an absolute measurement is not currently of a standard that could be used for essential management. Consequently we do not see sound as a method for absolute value monitoring, but rather a warning system, capable of detecting flood peaks when they occur or when the river might be starting to flood. If absolute

measurements are needed, alternative channel monitoring techniques are available.

Sound varied with stage in all the river reaches that we monitored, and so we are confident that noisy rivers will have a relationship with stage. The more data that are collected and correlated with the river stage, the greater the confidence we have in sound being used as a measurement. On reflecting on what makes a good section of river to monitor to measure sound, our Washburn data gave us ideas on sound generation from large obstacles, and making lots of noise was shown to be largely correct. Further work will need to be undertaken to allow an SPL–stage relationship to be predicted from the channel characteristics and without the need for previous stage data.

5 | CONCLUSION

At the start of this study, we set out to isolate river sound from a soundscape. The isolation of the river from the soundscape was achieved through the use of the LMF, which is capable of turning a poor, windy relationship into a promising, predictable signal. A perfect scenario, with no wind or rain noise, is still advantageous, but we have shown that even with these sources that river sound is a monitorable source of river stage information. Future work will need to be undertaken to allow stage measurements to be calculated without the need of calibration. The relationship between sound and a river's stage has been shown to have a strong relationship, with positive correlation seen in every site chosen. River morphology was shown to influence the sound that we were able to measure and from which to find relationships. Our results suggest that there is significant geomorphic control on sound production and that sound is unique to each river, like a fingerprint, but it is still able to be monitored after site calibration.

When assessing the usefulness of this technology, it has to be considered with regard to the benefits it may bring to places that require some sort of monitoring. The technology may not be used to determine an exact river stage, but to show if a flood peak has passed or if the river is rising or falling. Using sound as a method for measuring a river is a novel approach to remotely monitor rivers. Established methods of gathering hydrometric data are not going to be abolished thanks to this, but can work in harmony, with a larger catchment scale network envisioned, made up of several IoT devices that each work in their own specialised sector. Sound can fill the gaps where other hydrometric stations cannot be deployed, either due to infrastructure or cost. With continued research into this field, it may be possible to embed sound monitoring into a network-scale approach to river flood management, rather than isolating it to a sole source of information.

ACKNOWLEDGEMENTS

This work was supported by Durham University, the European Regional Development Fund–Intensive Industrial Innovation programme Grant No. 25R17P01847 and Evolto Ltd. We also acknowledge the help of the Environment Agency, from Victoria Crichton and John Lamb, and Yorkshire Water for their permission to monitor the River Washburn. The paper contains OS data © Crown copyright and database right 2021. We thank the anonymous reviewer for their invaluable comments and suggestions on the manuscript.

CONFLICTS OF INTEREST

There are no conflicts of interest.

DATA AVAILABILITY STATEMENT

The data that support the findings of this study are available from the corresponding author upon reasonable request.

ORCID

Wm. Alexander Osborne  <https://orcid.org/0000-0002-2168-8102>

Rebecca A. Hodge  <https://orcid.org/0000-0002-8792-8949>

Gordon D. Love  <https://orcid.org/0000-0001-5137-9434>

REFERENCES

- Anthony, R.E., Aster, R.C., Ryan, S., Rathburn, S. & Baker, M.G. (2018) Measuring mountain river discharge using seismographs emplaced within the hyporheic zone. *Journal of Geophysical Research: Earth Surface*, 123(2), 210–228.
- Bathurst, J.C. (2002) At-a-site variation and minimum flow resistance for mountain rivers. *Journal of Hydrology*, 269(1–2), 11–26.
- Bolghasi, A., Ghadimi, P. & Feizi Chekab, M.A. (2017) Sound attenuation in air–water media with rough bubbly interface at low frequencies considering bubble resonance dispersion. *Journal of the Brazilian Society of Mechanical Sciences and Engineering*, 39(12), 4859–4871.
- Burtin, A., Bollinger, L., Vergne, J., Cattin, R. & Nábélek, J.L. (2008) Spectral analysis of seismic noise induced by rivers: A new tool to monitor spatiotemporal changes in stream hydrodynamics. *Journal of Geophysical Research: Solid Earth*, 113(5), 1–14.
- Burtin, A., Cattin, R., Bollinger, L., Vergne, J., Steer, P., Robert, A. et al. (2011) Towards the hydrologic and bed load monitoring from high-frequency seismic noise in a braided river: The ‘torrent de St Pierre’, French Alps. *Journal of Hydrology*, 408(1–2), 43–53.
- Chacon-Hurtado, J.C., Alfonso, L. & Solomatine, D.P. (2017) Rainfall and streamflow sensor network design: A review of applications, classification, and a proposed framework. *Hydrology and Earth System Sciences*, 21(6), 3071–3091.
- Chanson, H. (1996) Free-surface flows with near-critical flow conditions. *Canadian Journal of Civil Engineering*, 23(6), 1272–1284.
- Chicharro, R. & Vazquez, A. (2014) The acoustic signature of gas bubbles generated in a liquid cross-flow. *Experimental Thermal and Fluid Science*, 55, 221–227.
- Comiti, F. & Lenzi, M.A. (2006) Dimensions of standing waves at steps in mountain rivers. *Water Resources Research*, 42(3): W03411.
- Eldwaik, O. & Li, F. (2018) Mitigating wind induced noise in outdoor microphone signals using a singular spectral subspace method. *Technologies*, 6(1), 19.
- Gaunard, G.C. & Überall, H. (1981) Resonance theory of bubbly liquids. *Journal of the Acoustical Society of America*, 69(2), 362–370.
- Geay, T., Belleudy, P., Gervaise, C., Habersack, H., Aigner, J., Kreisler, A. et al. (2017) Passive acoustic monitoring of bed load discharge in a large gravel bed river. *Journal of Geophysical Research: Earth Surface*, 122(2), 528–545.
- Govi, M., Maraga, F. & Moia, F. (1993) Seismic detectors for continuous bed load monitoring in a gravel stream. *Hydrological Sciences Journal*, 38(2), 123–132.
- Horii, Y., Hong, W., Tamaki, A. & Kitamura, T. (2018) Extraordinary acoustic transmission in human hearing system, Progress in Electromagnetics Research Symposium: Toyama, Japan.
- Klaus, M., Geibrink, E., Hotchkiss, E.R. & Karlsson, J. (2019) Listening to air–water gas exchange in running waters. *Limnology and Oceanography: Methods*, 17(7), 395–414.
- Krein, A., Schenkluhn, R., Kurtenbach, A., Bierl, R. & Barrière, J. (2016) Listen to the sound of moving sediment in a small gravel-bed river. *International Journal of Sediment Research*, 31(3), 271–278.
- Kruger, A., Krajewski, W.F., Niemeier, J.J., Ceynar, D.L. & Goska, R. (2016) Bridge-mounted river stage sensors (BMRSS). *IEEE Access*, 4, 8948–8966.
- Kucukali, S. & Cokgor, S. (2008) Boulder–flow interaction associated with self-aeration process. *Journal of Hydraulic Research*, 46(3), 415–419.
- Kumar, S. & Brennen, C.E. (1991) Nonlinear effects in the dynamics of clouds of bubbles. *Journal of the Acoustical Society of America*, 89(2), 707–714.
- Leighton, T. (1994) The sound field. In *The Acoustic Bubble*. Amsterdam: Elsevier.
- Leighton, T.G. (2012) How can humans, in air, hear sound generated underwater (and can goldfish hear their owners talking)? *Journal of the Acoustical Society of America*, 131(3), 2539–2542.
- Lin, I.-C., Hsieh, Y.-R., Shieh, P.-F., Chuang, H.-C. & Chou, L.-C. (2014) The effect of wind on low frequency noise. *Proceedings of INTER-NOISE 2014*, 1–12.
- Liu, Y., Jia, Y.B., Zhang, X.J., Liu, Z.C., Ren, Y.C. & Yang, B. (2013) Noise test and analysis of automobile engine. In: Gao, S. (Ed.) *Mechatronics and Computational Mechanics*, Vol. 307 of *Applied Mechanics and Materials*. Bach, Switzerland: Trans Tech, pp. 196–199.
- Manasseh, R., Babanin, A.V., Forbes, C., Rickards, K., Bobevski, I. & Ooi, A. (2006) Passive acoustic determination of wave-breaking events and their severity across the spectrum. *Journal of Atmospheric and Oceanic Technology*, 23(4), 599–618.
- Marsh, T.J. (2002) Capitalising on river flow data to meet changing national needs: A UK perspective. *Flow Measurement and Instrumentation*, 13(5–6), 291–298.
- Marsh, T. & Hannaford, J. (2008) *UK Hydrometric Register*. Centre for Ecology and Hydrology: Wallingford, UK.
- Mennitt, D. & Fristrup, K. (2012) Obtaining calibrated sound pressure levels from consumer digital audio recorders. *Applied Acoustics*, 73(11), 1138–1145.
- Minnaert, M. (1933) XVI. On musical air-bubbles and the sounds of running water. *London, Edinburgh, and Dublin Philosophical Magazine and Journal of Science*, 16(104), 235–248.
- Monson, B.B., Hunter, E.J., Lotto, A.J. & Story, B.H. (2014) The perceptual significance of high-frequency energy in the human voice. *Frontiers in Psychology*, 5, 587.
- Moreno, C., Aquino, R., Ibarreche, J., Pérez, I., Castellanos, E., Álvarez, E. et al. (2019) RiverCore: IoT device for river water level monitoring over cellular communications. *Sensors*, 19(1), 127.
- Morse, N., Bowden, W.B., Hackman, A., Pruden, C., Steiner, E. & Berger, E. (2007) Using sound pressure to estimate reaeration in streams. *Journal of the North American Benthological Society*, 26(1), 28–37.
- Muste, M., Fujita, I. & Hauet, A. (2008) Large-scale particle image velocimetry for measurements in riverine environments. *Water Resources Research*, 44(4), W00D19.
- Muste, M., Yu, K. & Spasojevic, M. (2004) Practical aspects of ADCP data use for quantification of mean river flow characteristics. Part I: Moving-vessel measurements. *Flow Measurement and Instrumentation*, 15(1), 1–16.
- Ohki, M., Zervakis, M.E. & Venetsanopoulos, A.N. (1995) 3-D Digital filters. *Control and Dynamic Systems*, 69, 49–88.
- Ronan, T.J., Lees, J.M., Mikesell, T.D., Anderson, J.F. & Johnson, J.B. (2017) Acoustic and seismic fields of hydraulic jumps at varying Froude numbers. *Geophysical Research Letters*, 44(19), 9734–9741.
- Schmandt, B., Aster, R.C., Scherler, D., Tsai, V.C. & Karlstrom, K. (2013) Multiple fluvial processes detected by riverside seismic and infrasound monitoring of a controlled flood in the Grand Canyon. *Geophysical Research Letters*, 40(18), 4858–4863.
- Schmandt, B., Gaeuman, D., Stewart, R., Hansen, S.M., Tsai, V.C. & Smith, J. (2017) Seismic array constraints on reach-scale bedload transport. *Geology*, 45(4), 299–302.
- Slabbekoorn, H. & Ripmeester, E.A. (2008) Birdsong and anthropogenic noise: Implications and applications for conservation. *Molecular Ecology*, 17(1), 72–83.

- Tonolla, D., Lorang, M.S., Heutschi, K. & Tockner, K. (2009) A flume experiment to examine underwater sound generation by flowing water. *Aquatic Sciences*, 71(4), 449–462.
- Withers, M.M., Aster, R.C., Young, C.J. & Chael, E.P. (1996) High-frequency analysis of seismic background noise as a function of wind speed and shallow depth. *Bulletin of the Seismological Society of America*, 86(5), 1507–1515.
- Yackinous, W.S. (2015) Characteristics of ecological network dynamics. In: Yackinous, W.S. (Ed.) *Understanding Complex Ecosystem Dynamics*. Boston, MA: Academic Press, pp. 265–298.

How to cite this article: Osborne, W.A., Hodge, R.A., Love, G. D., Hawkin, P. & Hawkin, R.E. (2021) Babbling brook to thunderous torrent: Using sound to monitor river stage. *Earth Surface Processes and Landforms*, 46(13), 2656–2670. Available from: <https://doi.org/10.1002/esp.5199>